# Symmetry energy from electromagnetic properties of exotic nuclei

TECHNISCHE UNIVERSITÄT DARMSTADT

**International Workshop XLVIII on Gross Properties of Nuclei and Nuclear Excitations**

**Hirschegg, Austria, January 12-18, 2020**

**Dominic Rossi**

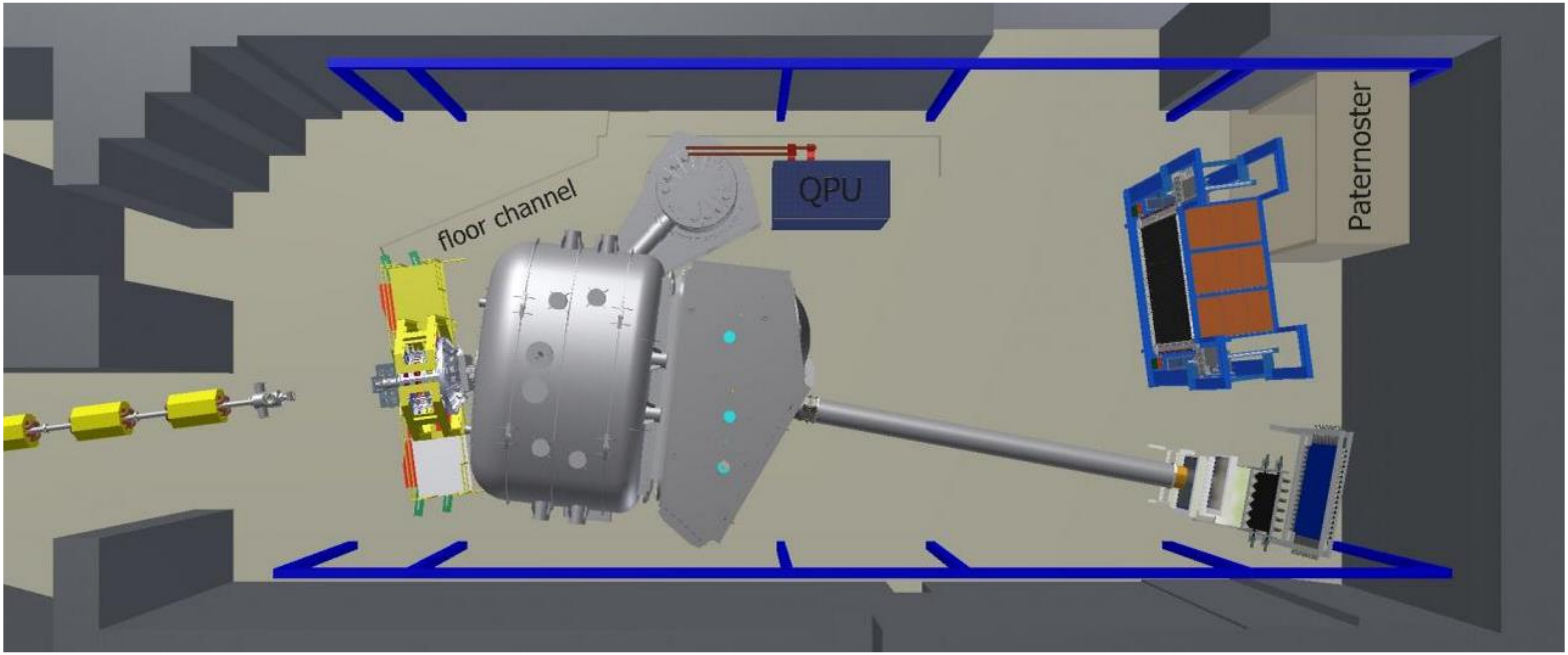

# Outline

- Introduction
  - EOS, symmetry energy and observables
- Dipole polarizability and how to measure it
- Influence of decay and detector response
- Dipole polarizability of $^{68,70}$Ni (above n threshold)
- E1 strength of $^{132}$Sn below n threshold
- Outlook:
  - Improving setup response
  - Using charge radii to constrain the symmetry energy

# Nuclear Equation of State

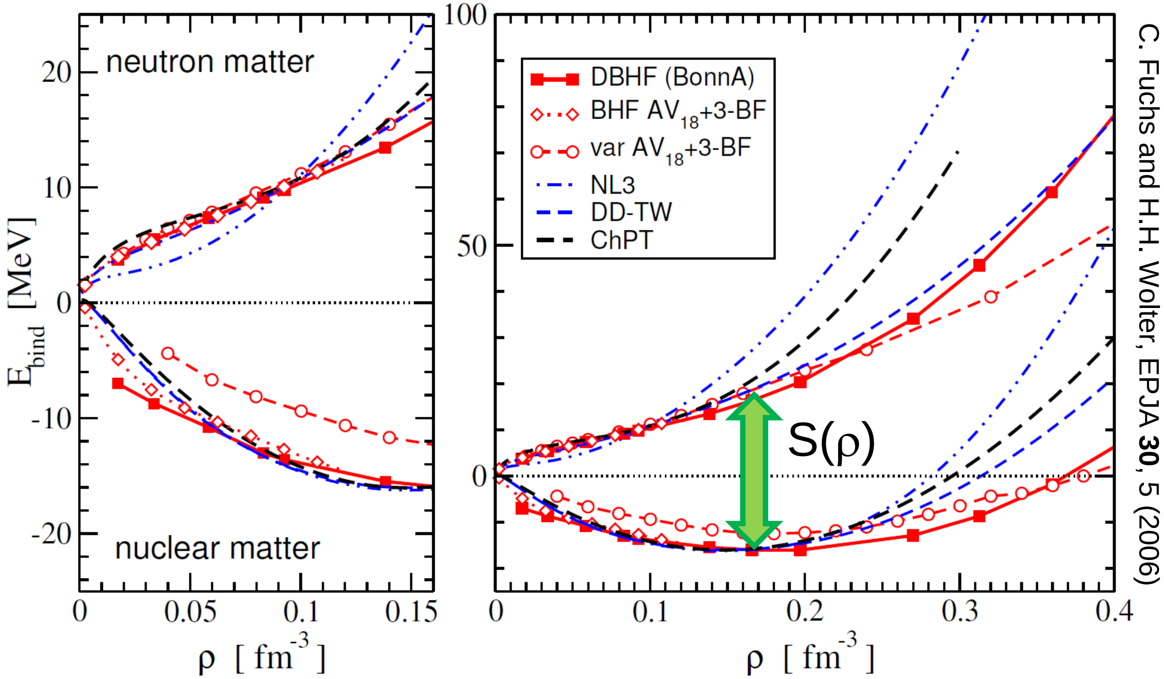


- Two extremes:
  - α = 0: symmetric matter
  - α = 1: neutron matter
- Symmetry energy: difference between symmetric and neutron matter, at a given density
- Good experimental constraints for symmetric nuclear matter exist (experiments with stable nuclei)

$$E(\rho,\alpha) = E(\rho,0) + S(\rho)\alpha^2 + \mathcal{O}(\alpha^4)\text{, with } \alpha = \frac{N-Z}{A}$$

$$S(\rho) \approx J + L\epsilon(\rho) + \frac{1}{2}K_{sym}\epsilon^2(\rho) \qquad \epsilon(\rho) = \frac{\rho-\rho_{sat}}{3\rho_{sat}}$$

# Nuclear symmetry energy parameters

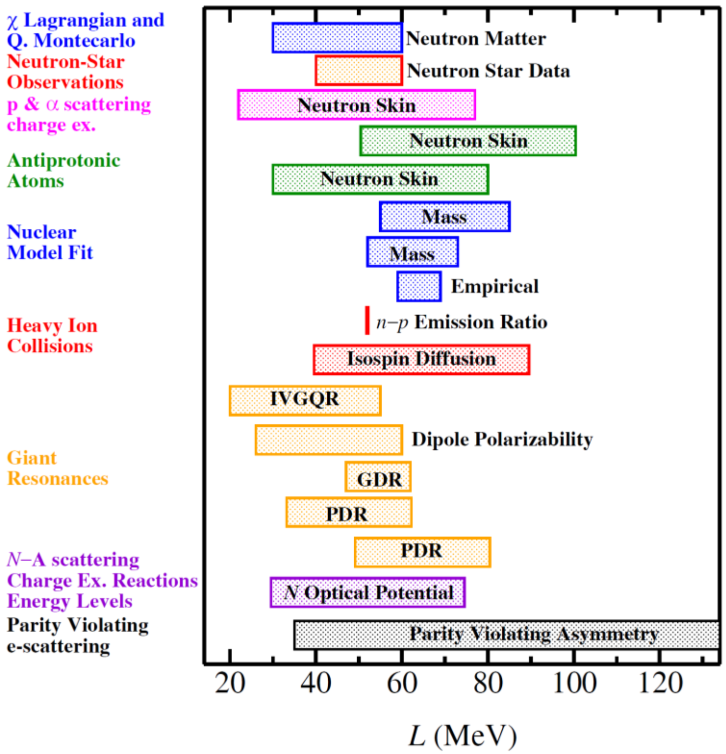


X. Vinas, *et al.*, EPJA **50**, 50 (2014)

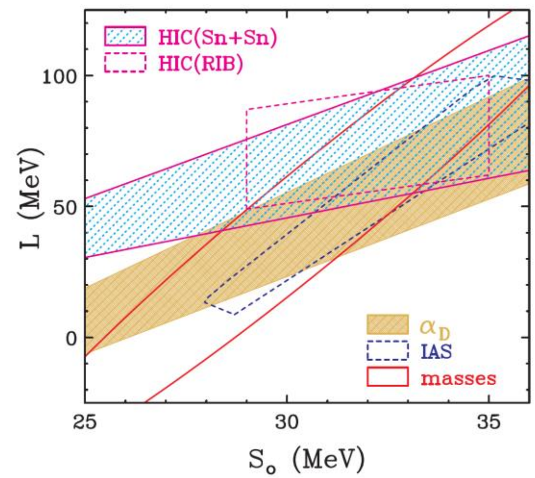


C. Horowitz, *et al.*, JPG **41**, 093001 (2014)

$$S(\rho) = J - L\frac{\rho - \rho_0}{3\rho_0} + \mathcal{O}(\rho^2)$$

- Symmetry energy J (at saturation density) is reasonably well constrained (masses, reactions, giant resonances, n-stars) between 30 and 35 MeV
- Slope parameter L still elusive
- 20 MeV ≤ L ≤ 120 MeV

# Choosing the “right” observable

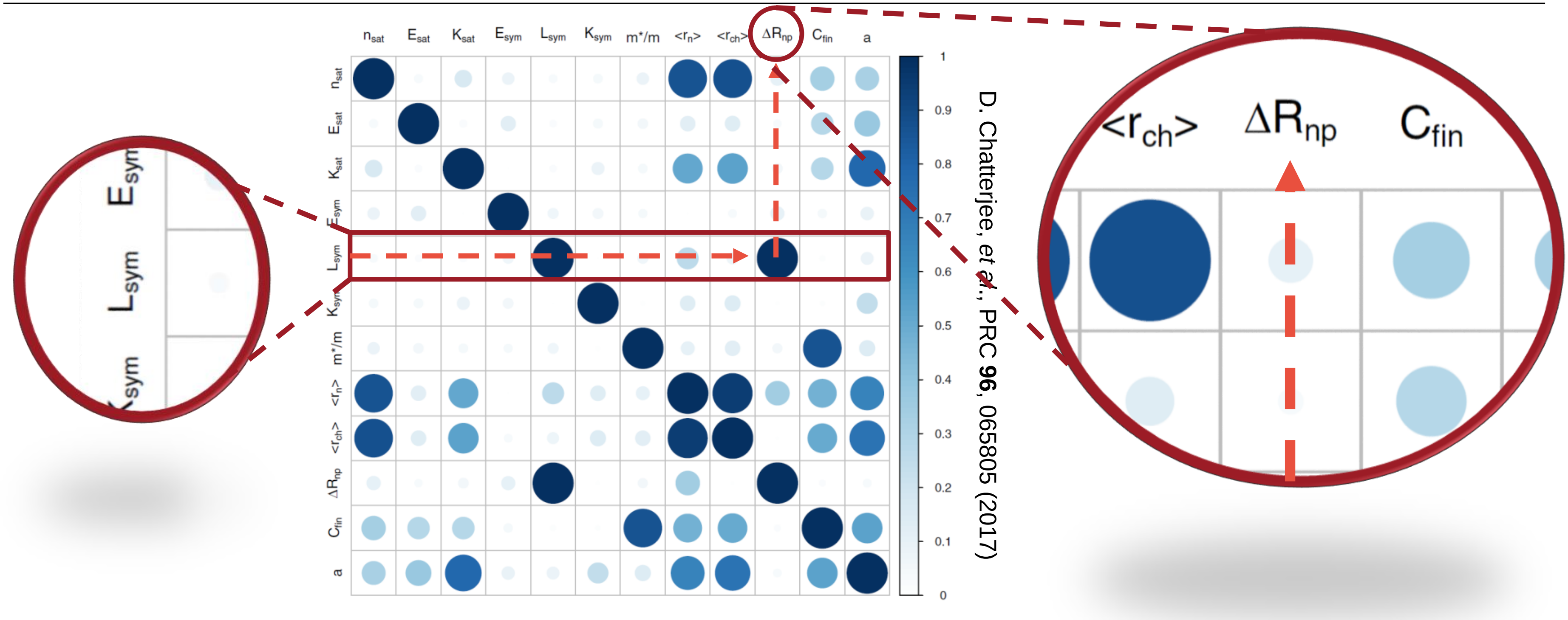


D. Chatterjee, *et al.*, PRC **96**, 065805 (2017)

- Calculations provide correlation matrices of various EOS parameters and observable quantities
- Identify parameter/observable pairs with strongest possible correlations

# Choosing the “right” observable

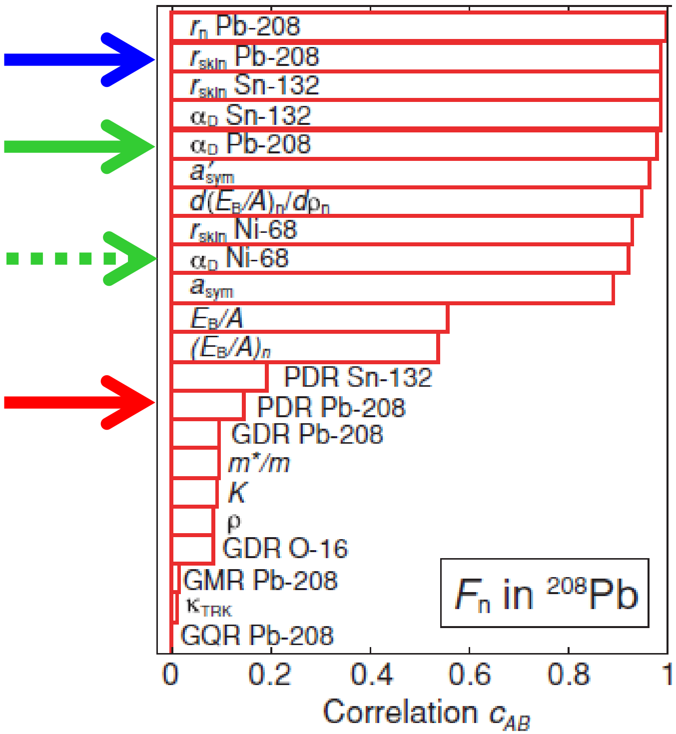


P.-G. Reinhard and W. Nazarewicz, PRC **81**, 051303(R) (2010)

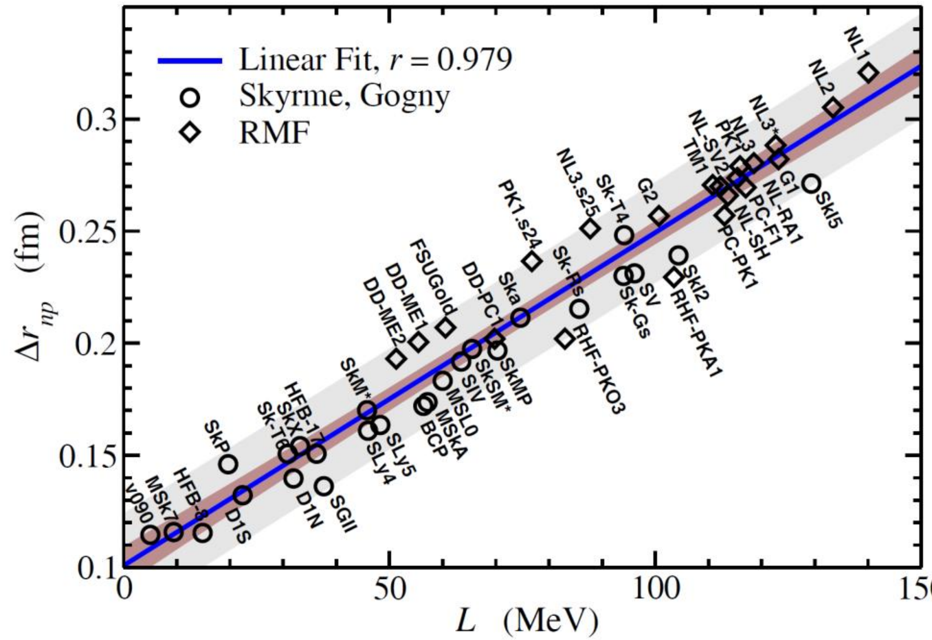


X. Vinas, *et al.*, EPJA **50**, 50 (2014)

- Example of $\Delta R_{n,p}$ vs. L correlation
- Skyrme, Gogny and RMF families show same linear correlation
- Reduced model dependence by considering multiple interaction families at same time
- Provides theoretical uncertainty in addition to experimental one

# Why use unstable isotopes for EOS studies?

- Possibility to change asymmetry ($\frac{N-Z}{A}$) over a much smaller mass range
- Study isotopic or isotonic chains (only change either N or Z)

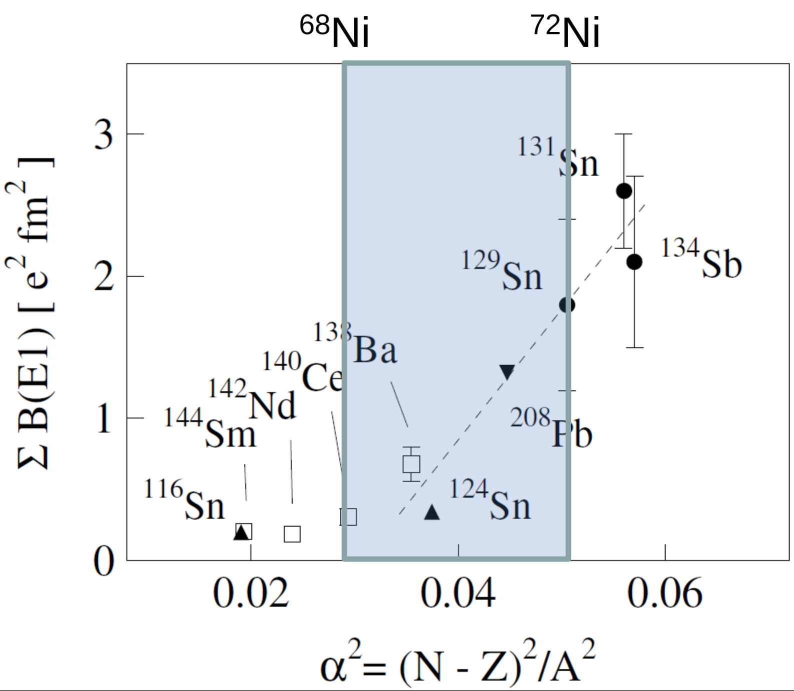


A. Klimkiewicz, *et al.*, PRC **76**, 051603(R) (2007)

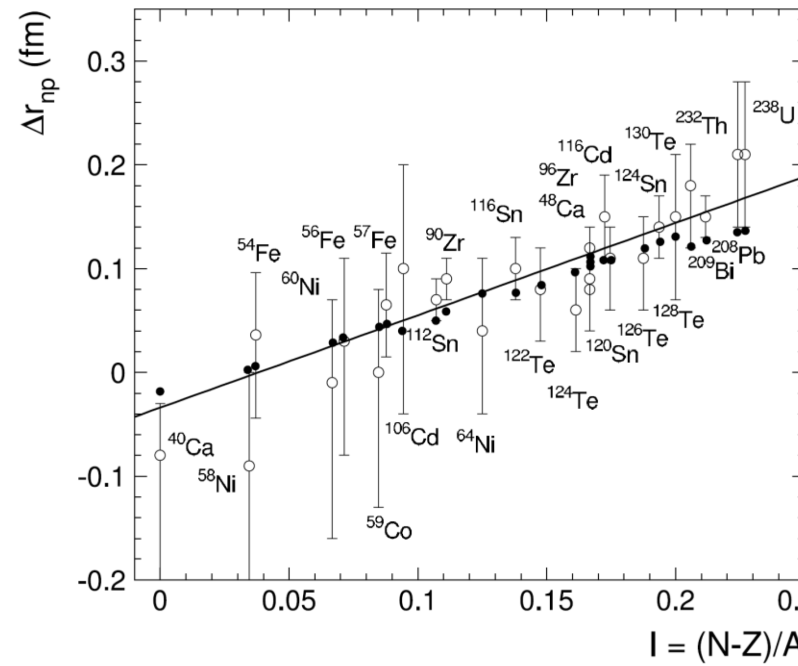


W.J. Swiatecki, *et al.*, PRC **71**, 047301 (2005)

- Some nuclear effects only appear beyond a certain asymmetry

➔ Add a second degree of freedom in choice of nucleus

# Dipole polarizability

TECHNISCHE UNIVERSITÄT DARMSTADT

$^{208}$Pb

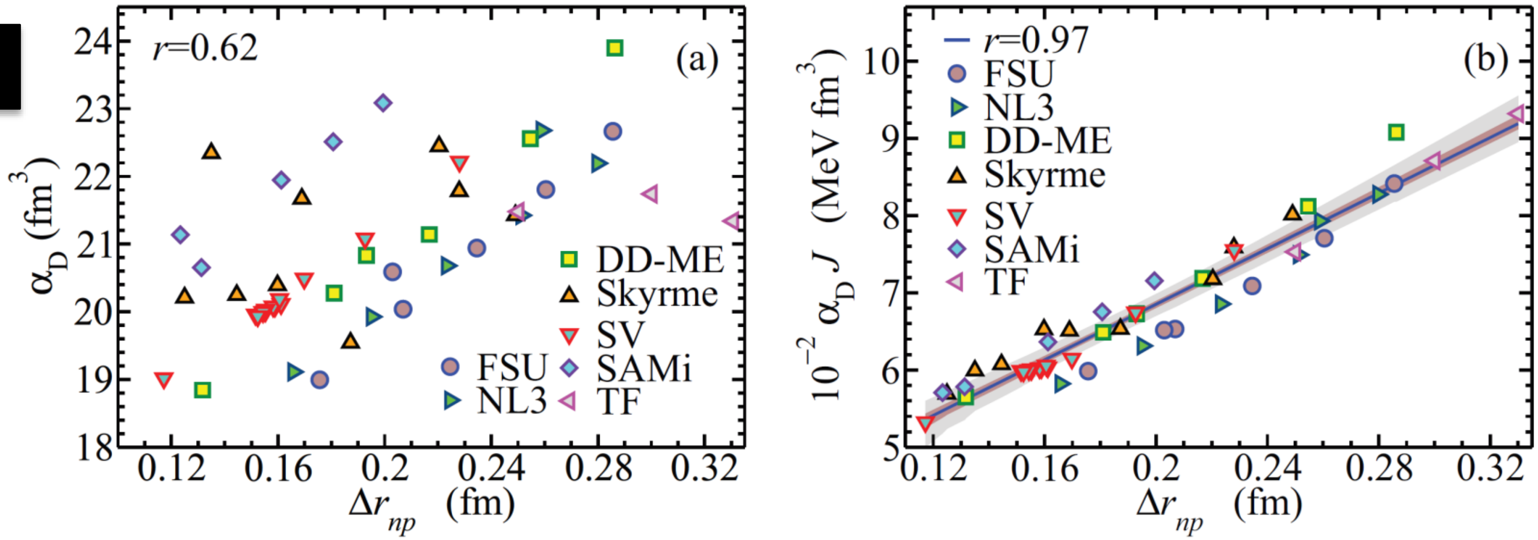


X. Roca-Maza, *et al.*, PRC **88**, 024316 (2013)

$$\alpha_D^{\mathrm{DM}} \approx \frac{\pi e^2}{54} \frac{A\langle r^2 \rangle}{J} \left[ 1 + \frac{5}{3} \frac{L}{J} \epsilon_A \right]$$

- Dipole polarizability and n-skin thickness of various interaction families each have own linear correlation
- The product $\alpha_D$*J reveals a less model-dependent correlation



R3B

# Dipole polarizability of $^{208}$Pb

PRL **107,** 062502 (2011) PHYSICAL REVIEW LETTERS week ending 5 AUGUST 2011

**Complete Electric Dipole Response and the Neutron Skin in $^{208}$Pb**

A. Tamii,[1] I. Poltoratska,[2] P. von Neumann-Cosel,[2,*] Y. Fujita,[3] T. Adachi,[3,4] C. A. Bertulani,[5] J. Carter,[6] M. Dozono,[7] H. Fujita,[1] K. Fujita,[7] K. Hatanaka,[1] D. Ishikawa,[1] M. Itoh,[8] T. Kawabata,[9] Y. Kalmykov,[2] A. M. Krumbholz,[2] E. Litvinova,[10,11] H. Matsubara,[12] K. Nakanishi,[12] R. Neveling,[13] H. Okamura,[1] H. J. Ong,[1] B. Özel-Tashenov,[10] V. Yu. Ponomarev,[2] A. Richter,[2,14] B. Rubio,[15] H. Sakaguchi,[1] Y. Sakemi,[8] Y. Sasamoto,[12] Y. Shimbara,[3,16] Y. Shimizu,[17] F. D. Smit,[13] T. Suzuki,[1] Y. Tameshige,[18] J. Wambach,[2] R. Yamada,[16] M. Yosoi,[1] and J. Zenihiro[1]

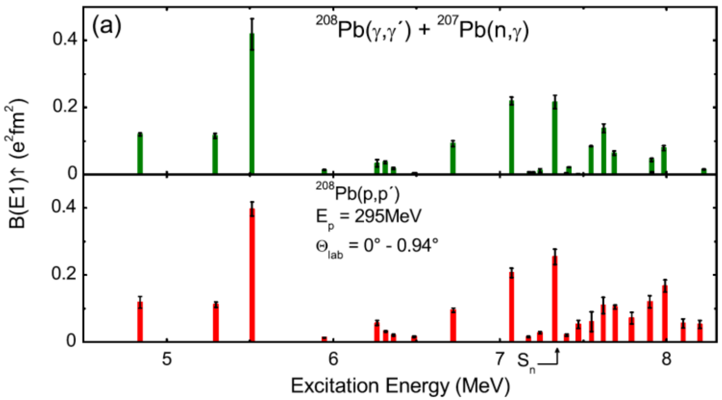


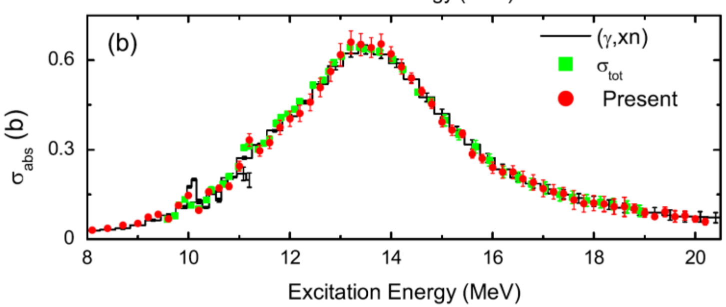


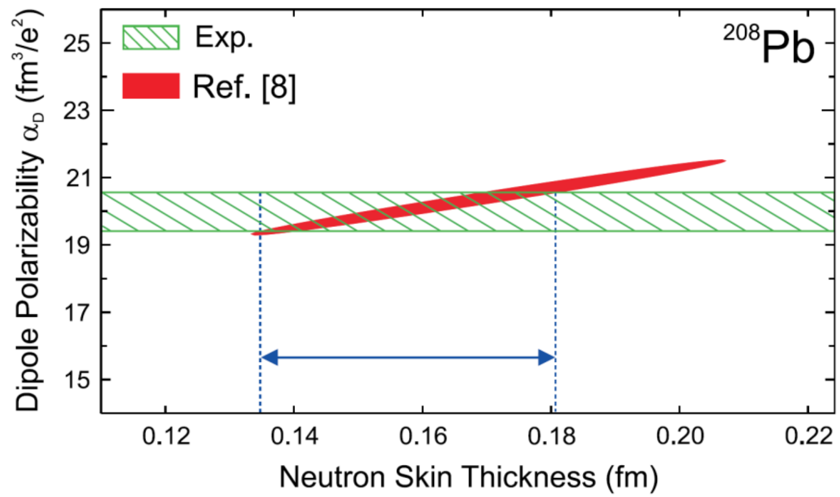


Measured $\alpha_D$ up to 20 MeV: 18.9(13) fm$^3$/e$^2$
Extrapolated value up to 130 MeV: 20.1(6) fm$^3$/e$^2$
➔ $r_{\rm skin} = 0.156^{+0.025}_{-0.021}$ fm

# Measuring E1 strength in unstable nuclei

TECHNISCHE UNIVERSITÄT DARMSTADT

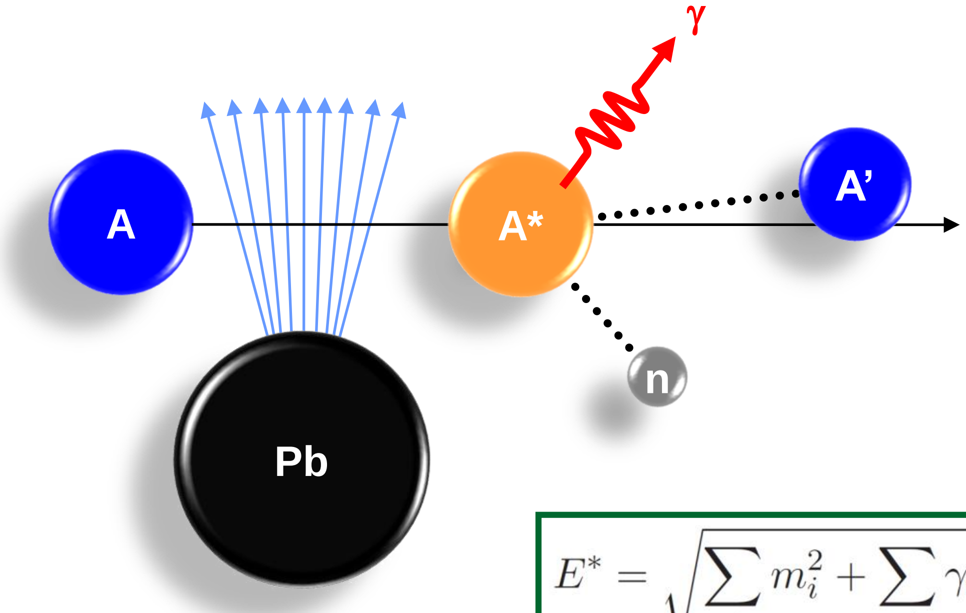


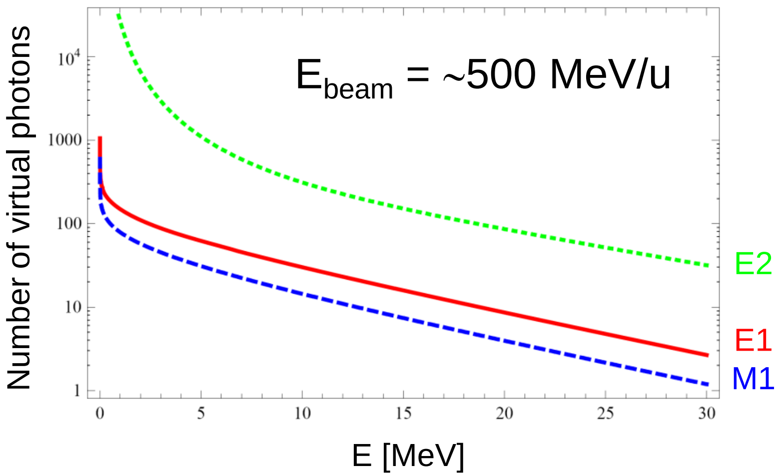


$$E^* = \sqrt{\sum_i m_i^2 + \sum_{i \neq j} \gamma_i \gamma_j m_i m_j \left(1 - \beta_i \beta_j \cos\vartheta_{ij}\right)} + E_\gamma - m_{proj}$$

- Short lifetime of projectile ➔ requires experiment in **inverse kinematics**
- Heavy-ion-induced **electromagnetic excitation**, *via* the virtual photon approach
- Reconstruction of excitation energy (using invariant mass) of each event requires detection of **ALL** participating species (identification and momentum):
  ➔ Requires high-efficiency and high-resolution neutron and gamma detectors (for n-rich nuclei)



R3B

# GSI and FAIR complex

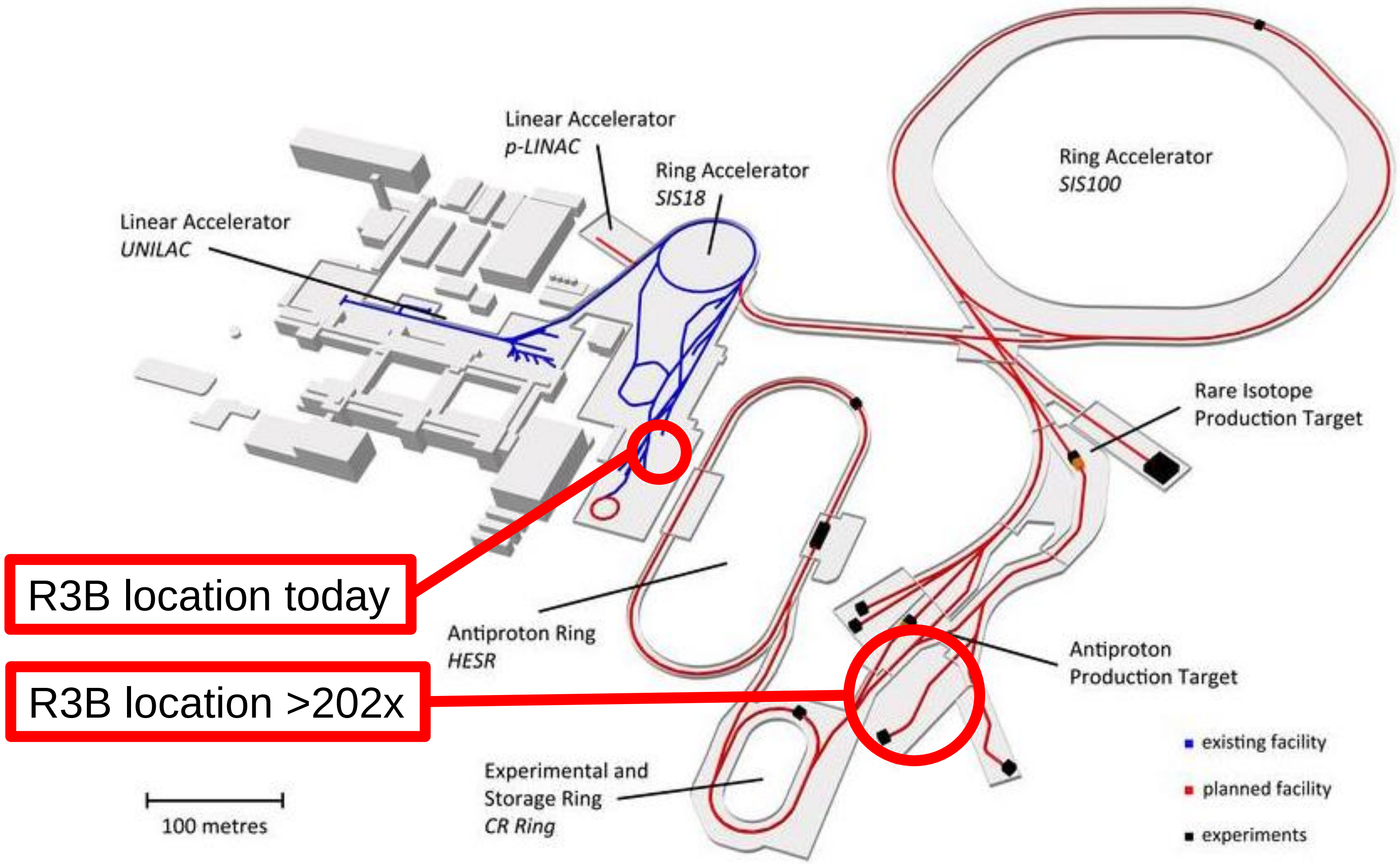

# $R^3B$ Overview

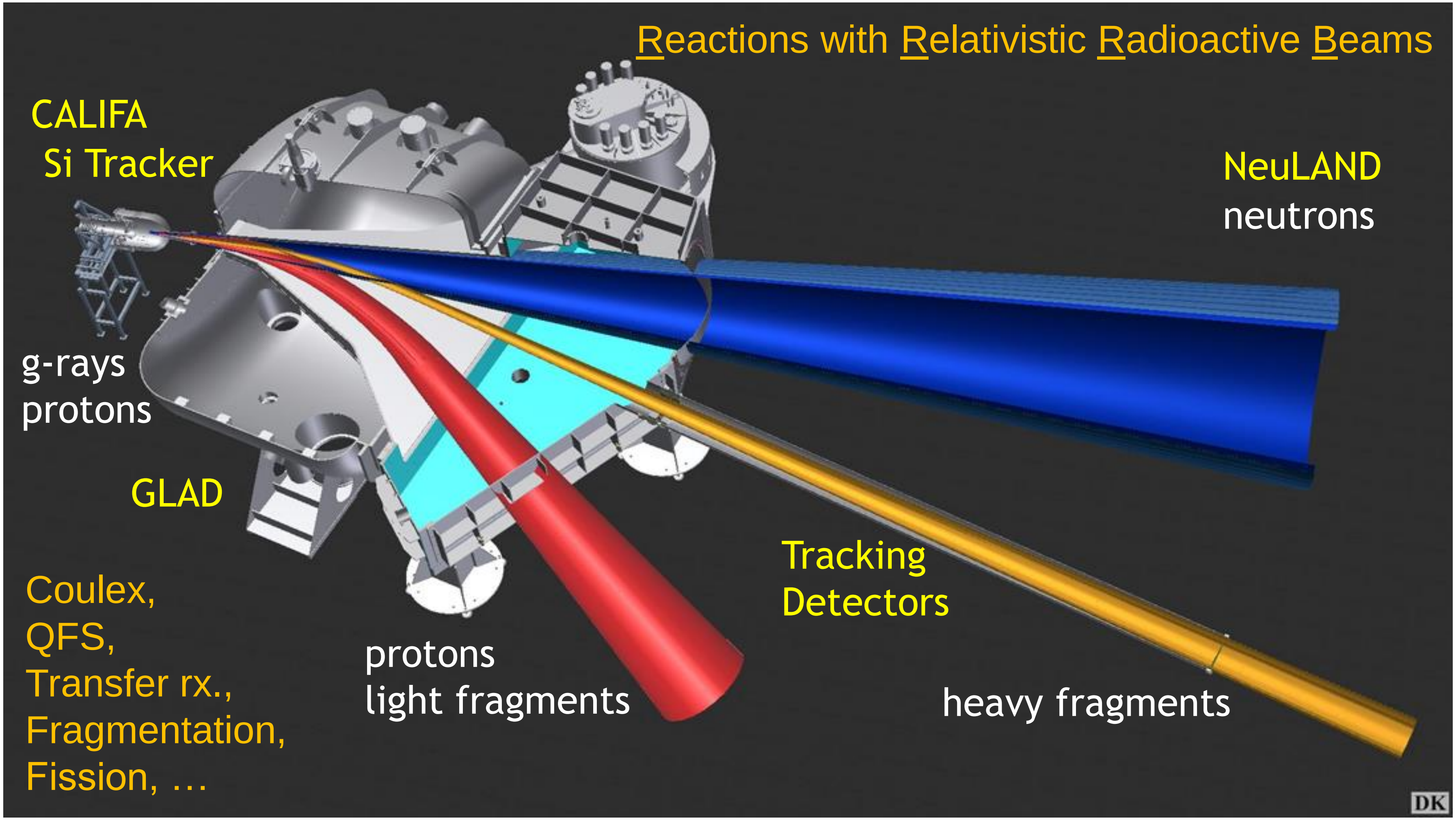

# Determine full $\alpha_D$ for $^{68}$Ni

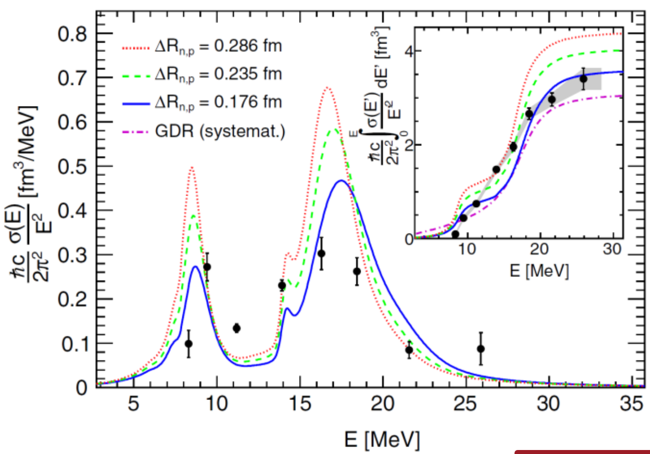


D.M. Rossi, *et al.*, PRL **111**, 242503 (2013)

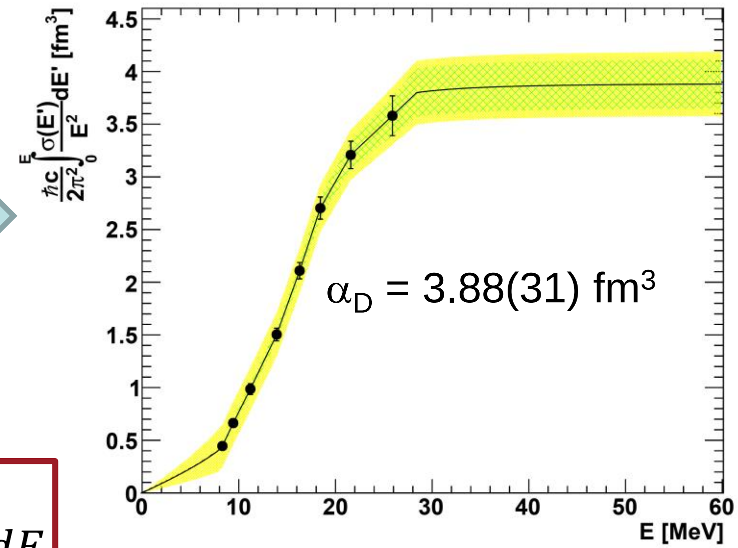


$$\alpha_D = \frac{\hbar c}{2\pi^2}\int_0^\infty \frac{\sigma(E)}{E^2}\,dE$$

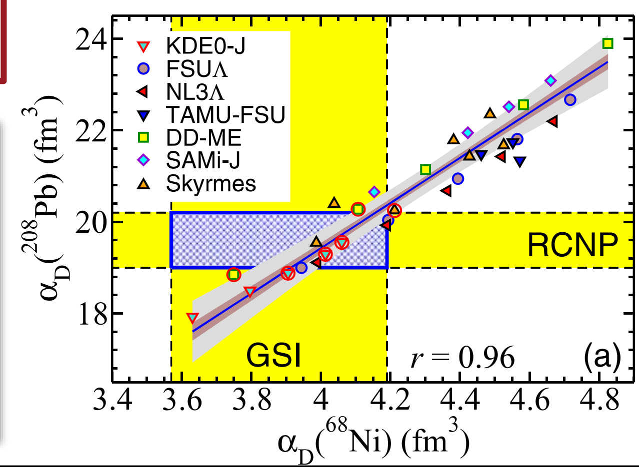


X. Roca-Maza, *et al.*, PRC **92**, 064304 (2015)

- Measurement from $S_n$ up to 28.4 MeV
- Expand integration range from 7.792-28.4 MeV to 0-140 MeV
- Use Breit-Wigner tails from fit to data to extrapolate E1 strength beyond measurement range
- Reflect extrapolation in total error

# Influence of decay properties

TECHNISCHE UNIVERSITÄT DARMSTADT

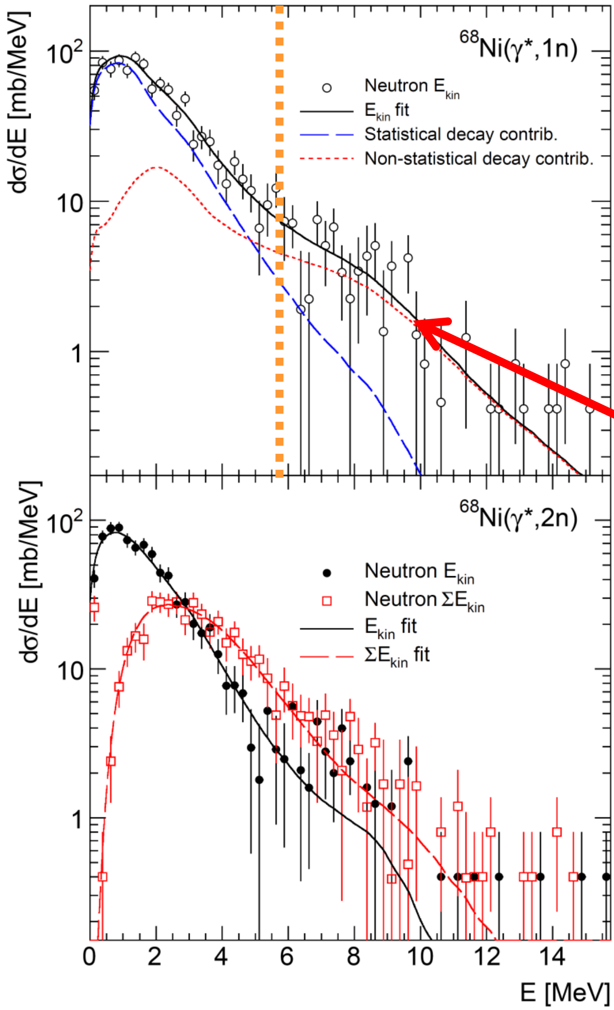


- Neutron kinetic energies reach well beyond the 2n threshold (dotted orange line)

→ Not expected with statistical decay

- Only decay to the vicinity of the A-1 ground state was considered
- Non-statistical decay branching ratio obtained from fit to neutron energies

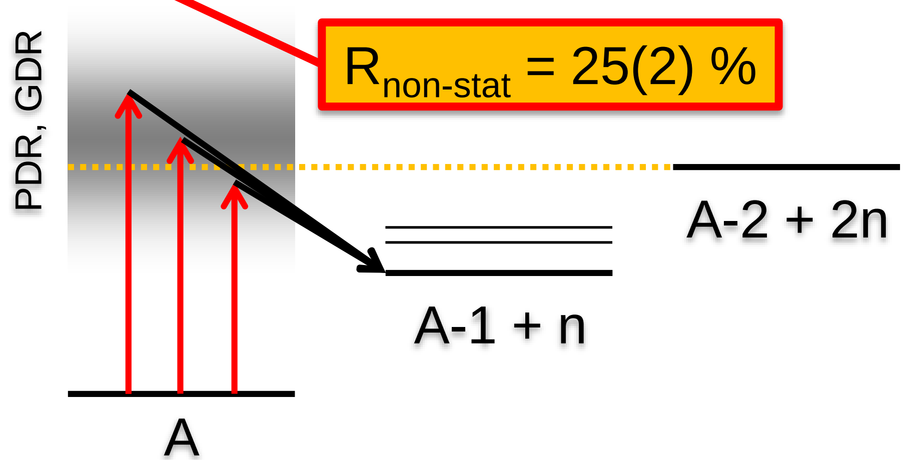




R³B

# Influence of neutron detection

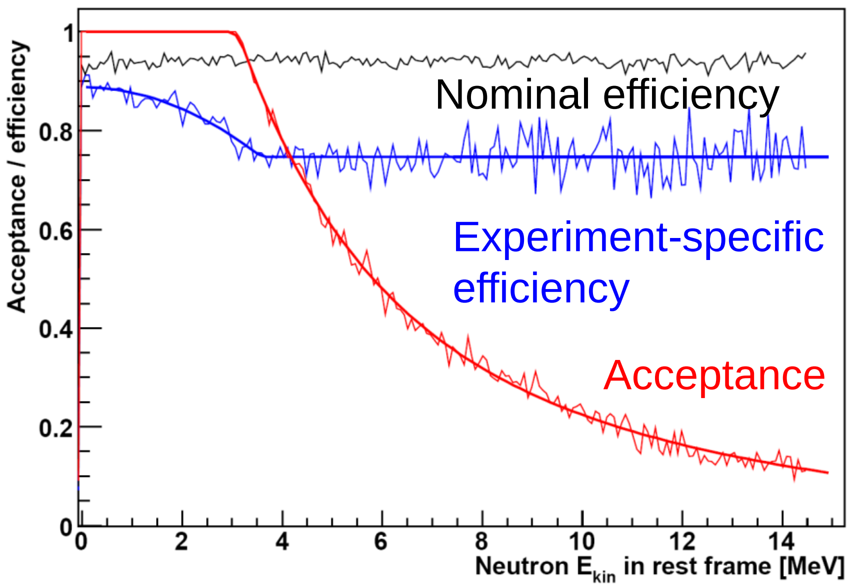


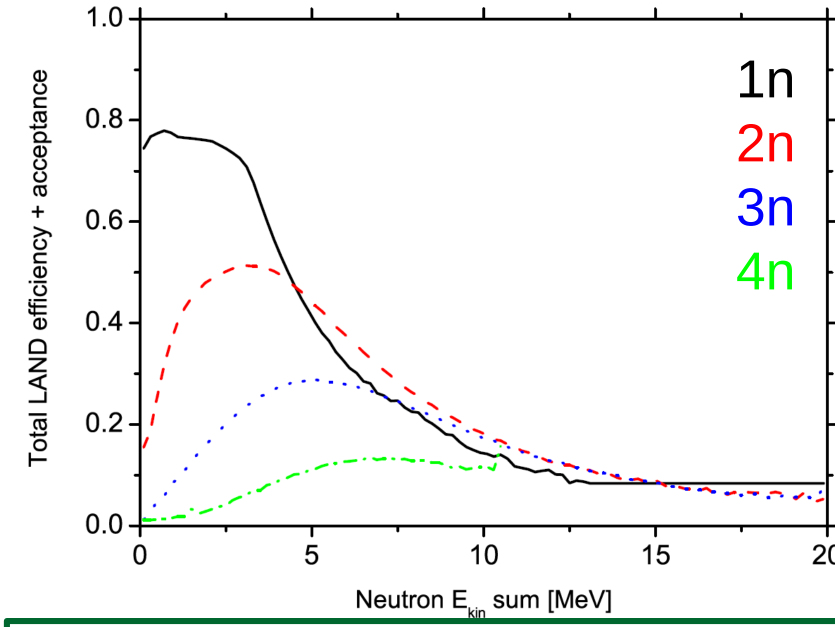


- Experimental data can be corrected for LAND acceptance and efficiency
- Nominal efficiency: determined by $^{2}H$ experiment
- Experiment-specific efficiency: depends on dead and semi-dead paddles
- Acceptance: depends on the kinetic energy of the neutrons

- Total efficiency + acceptance curves for 1n to 4n channels
- Sum of neutron kinetic energies sufficiently good observable
- Loss of detection efficiency at low E due to overlapping hit distributions
- Experimental data corrected with these functions

# Influence of gamma detection

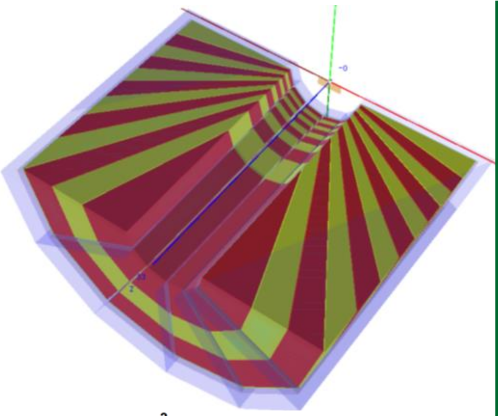

- Simulation of CsI with:
  - Clustering algorithm with add-back
  - Doppler correction
- Source moving with $\beta \approx 0.75$
- Plot shows cluster sum energy ➔ should ideally show peak at 2.67 MeV
- Large probability to only see one photon (two peaks around 1-1.5 MeV)

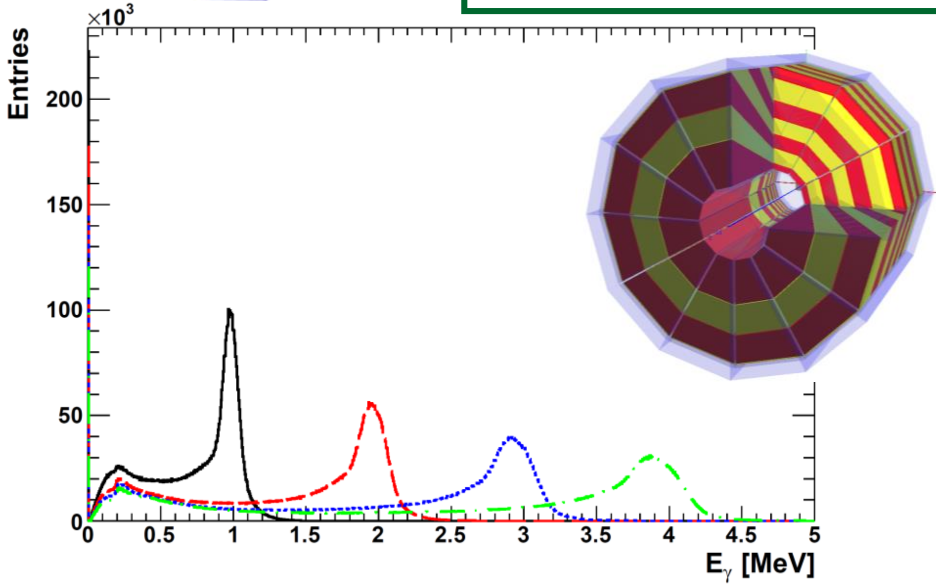


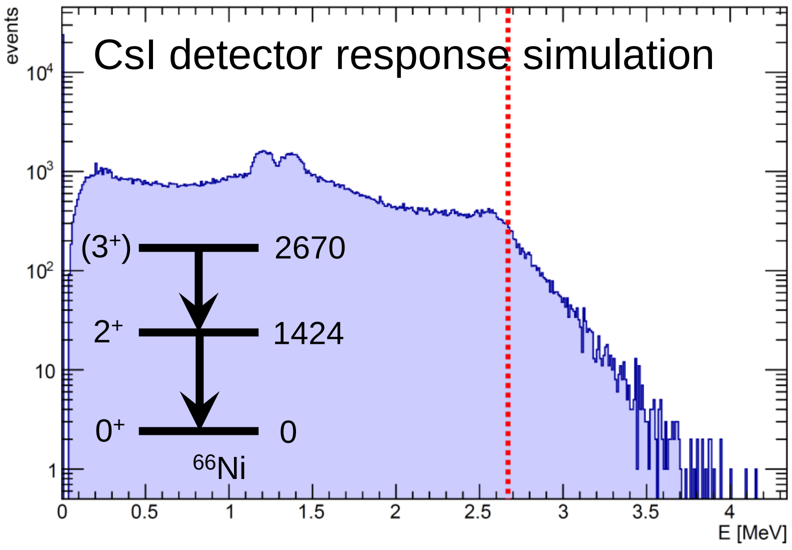

# Experimental setup response function

$$\left(\frac{d\sigma_C}{dE_{invm}}\right)(E_{invm}) = \sum_{i=1}^{4}\sum_{j=1}^{3}\int_{E^*}\mathcal{R}\left(i,j,E^*,E_{invm}\right)\cdot\mathcal{B}\left(i,E^*\right)\cdot\mathcal{M}\left(i,j\right)\cdot\left(\frac{d\sigma_C}{dE^*}\right)(E^*)\,dE^*$$

Example for $^{68}Ni(\gamma^*,2n)^{66}Ni$

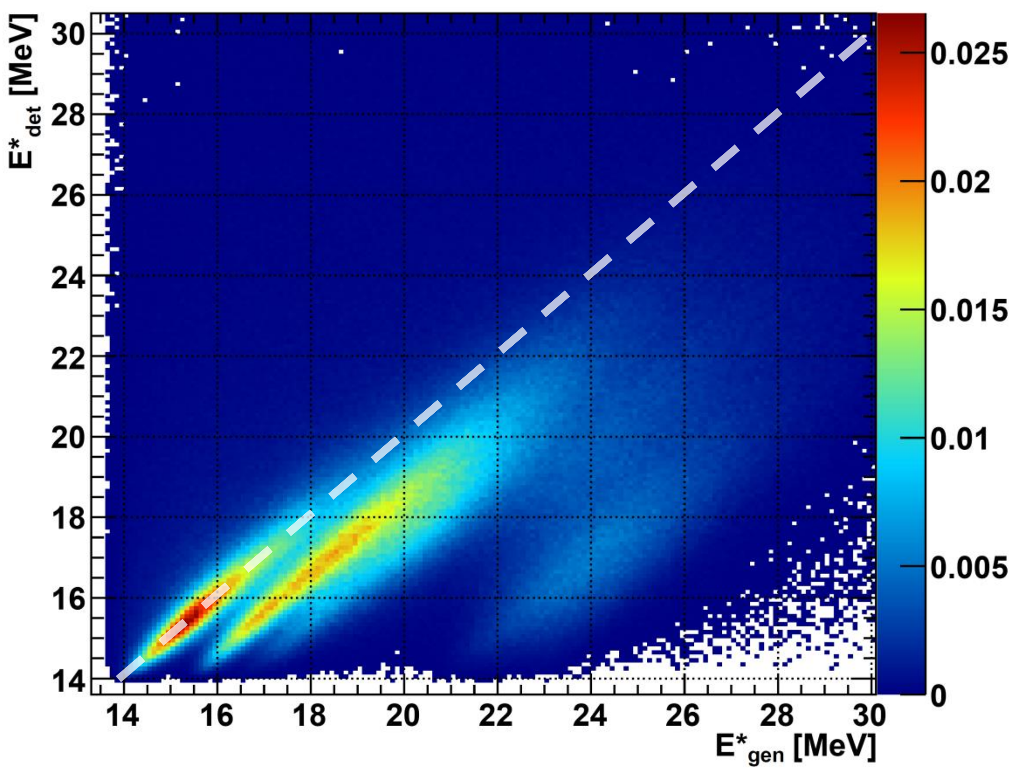


- Strong experimental response (broadening + distortion) due to complex (and inefficient) detectors
- Removal of response requires precise response matrices
- One matrix per channel and observable
- Iterative procedure
  - Folding of trial input
  - Calculate $\chi^2$ from comparison with data
  - Adjustment of trial input

# Fitting experimental data

TECHNISCHE UNIVERSITÄT DARMSTADT

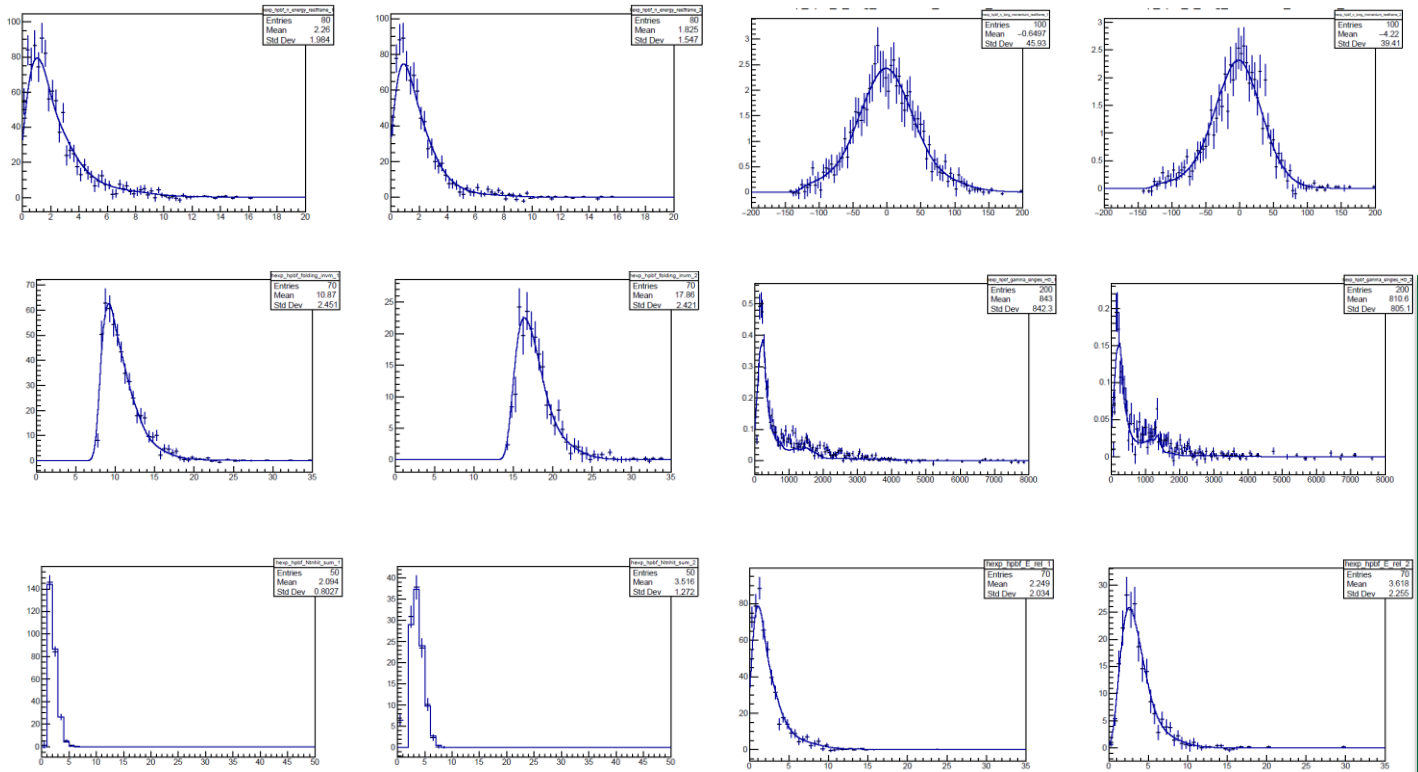

Fit ingredients:

- $E^*$
- Momentum distr.
- Neutron $E_{kin}$
- Neutron $\Sigma E_{kin}$
- $\gamma$ singles
- $\gamma$ sum
- Neutron hit mult.
- $\gamma$ multiplicity
- $E_{rel}$

Simultaneous fit to multiple distributions for all neutron channels



R3B

# Bin-wise deconvolution ($^{68}Ni$)

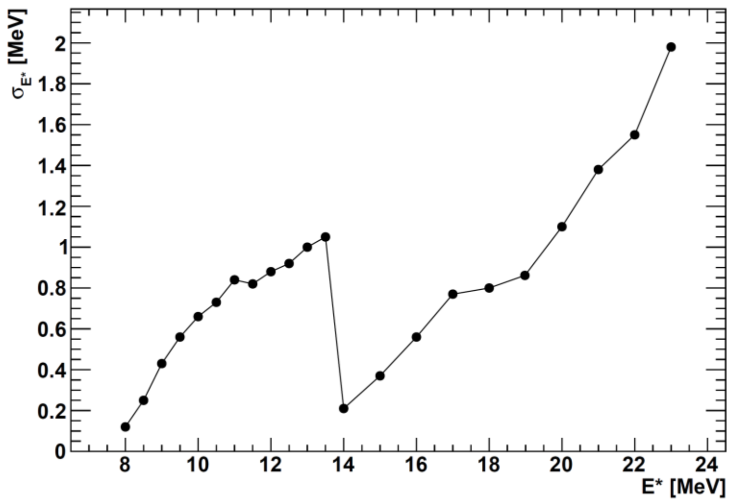


- Bin widths adjusted to E* resolution
- Scaling of $\sigma_{E*}$ and addition of minimal and maximal bin widths to probe bias from binning scheme
- Random scaling of parameters leads to $\alpha_D$ running sum band
- Red data points: fit with best $\chi^2$
- Blue data points: published values

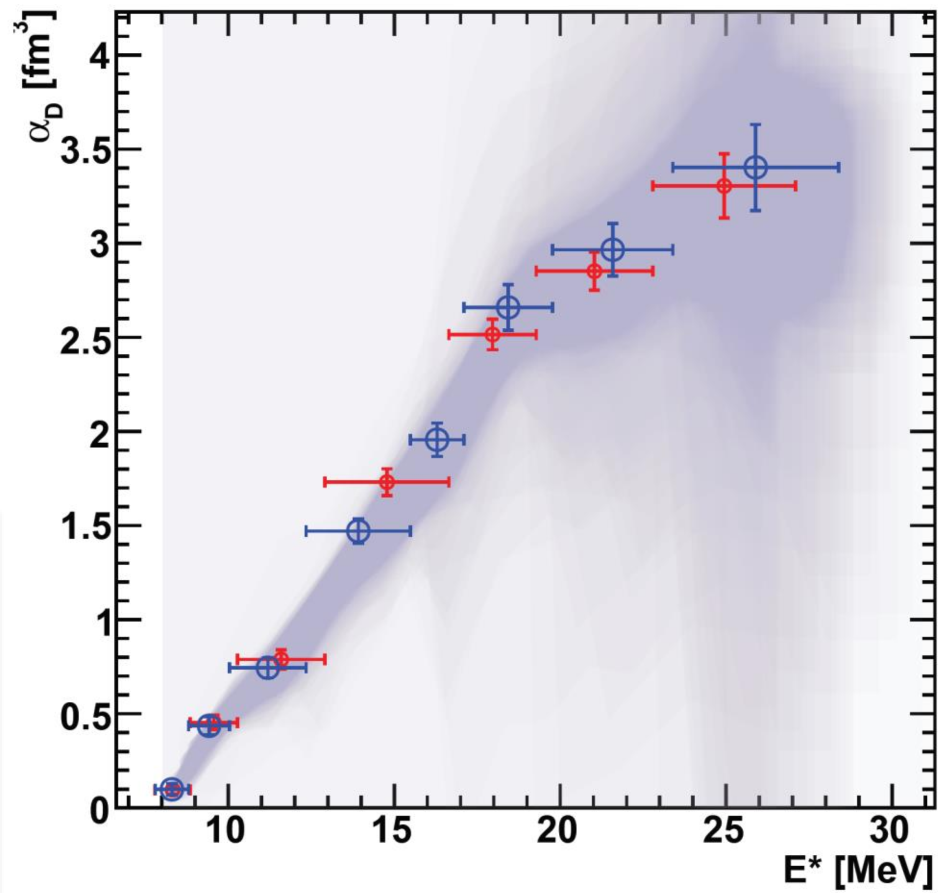

# Experimental challenges: multiple neutron detection

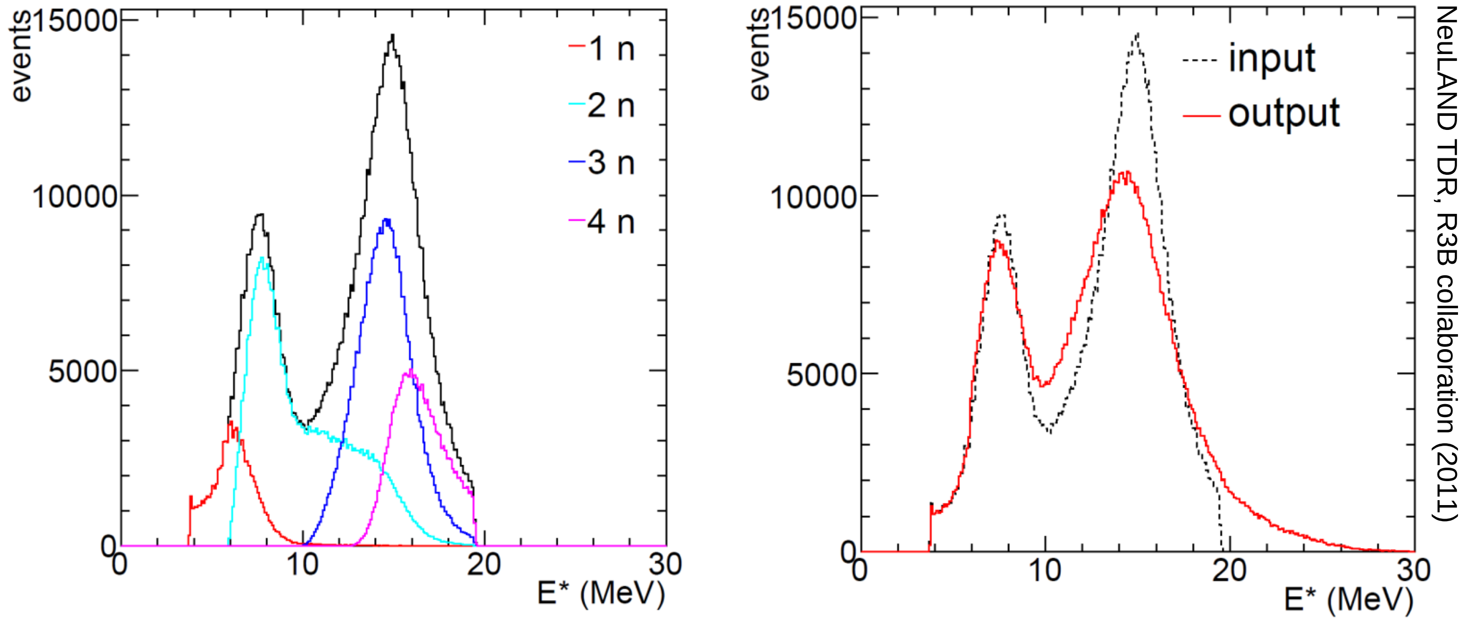


- Head towards more exotic systems → greater proton/neutron asymmetry
- Will require efficient multi-neutron detection capabilities
- Example for $^{136}Sn$@1 GeV/nucleon using NeuLAND, assuming 100% calorimetric efficiency of gamma detector (full CALIFA detector)

# Experimental challenges: multiple photon detection



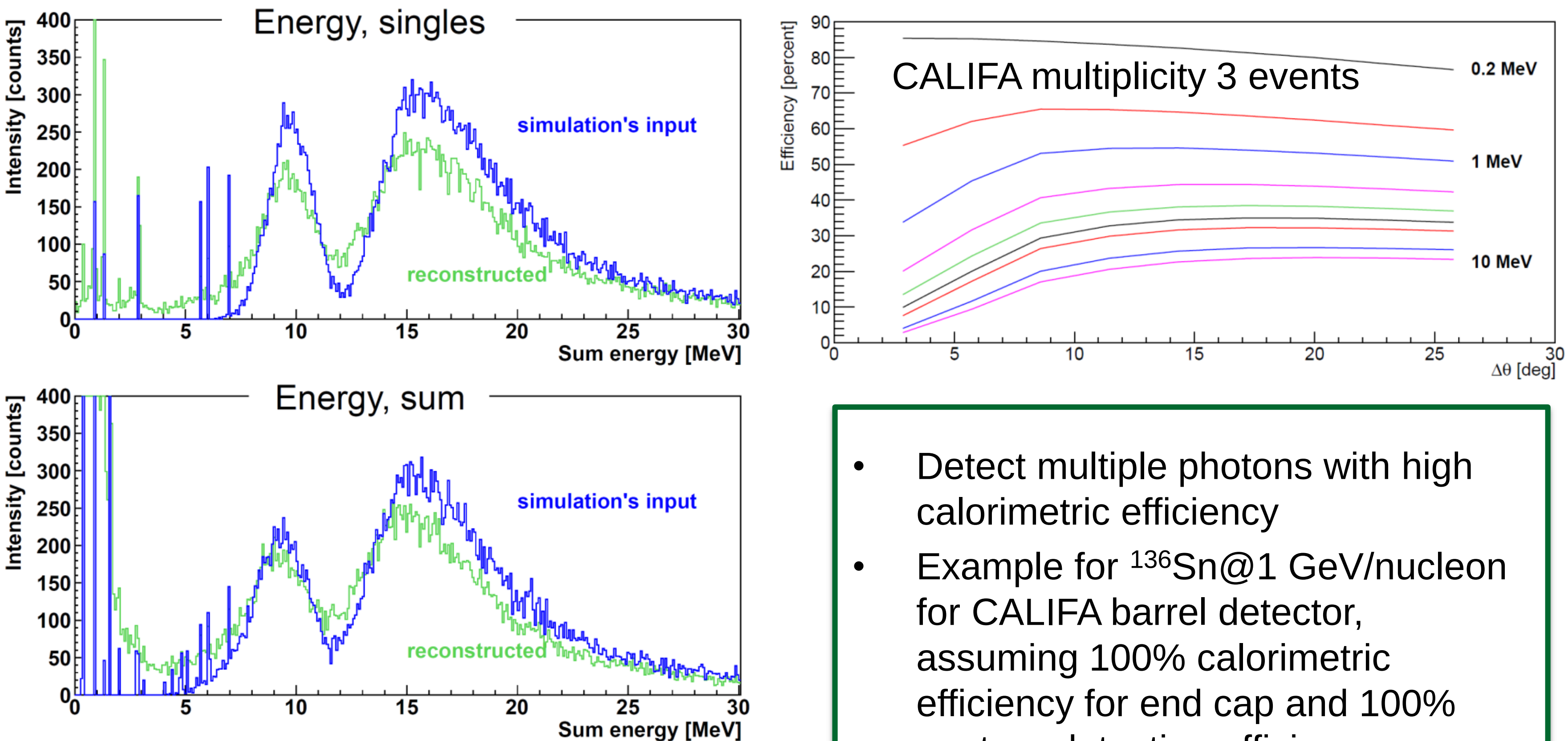


- Detect multiple photons with high calorimetric efficiency
- Example for $^{136}Sn$@1 GeV/nucleon for CALIFA barrel detector, assuming 100% calorimetric efficiency for end cap and 100% neutron detection efficiency

CALIFA Barrel TDR, R3B collaboration (2011)

# CALIFA: CALorimeter for In Flight detection of gamma rays and high-energy charged pArticles

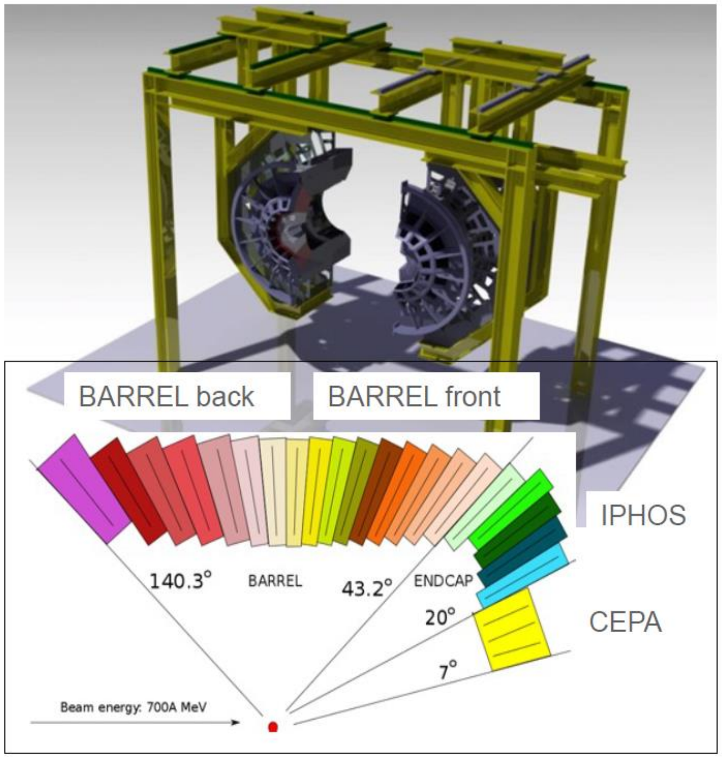


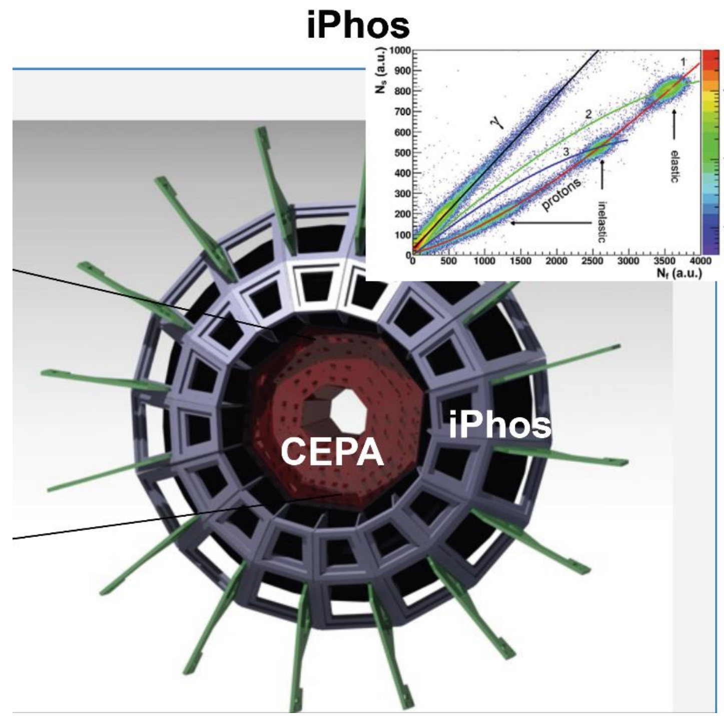


CALIFA barrel:

- Total of 1952 CsI(Tl) crystals (1152 in front half)
- Barrel mounted in Cave C for 2020 beam

- CEPA (CsI(Tl)) and iPhos ($LaBr_3$/$LaCl_3$) in testing phase
- Completion expected >2020

# NeuLAND

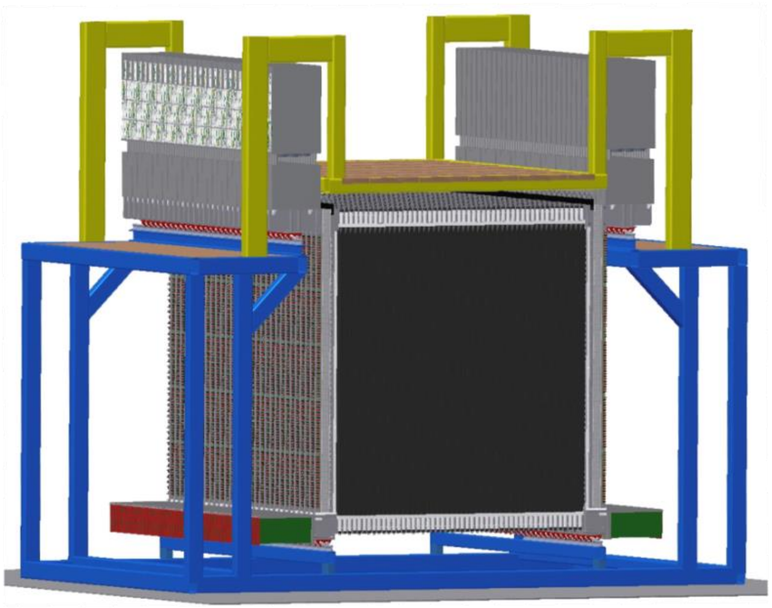

## NeuLAND detector parameters:

- full active detector using RP/BC408
- face size 250x250 $cm^2$
- active depth 300 cm
- 3000 scintillator bars + 6000 PMTs
- 32 tons
- $\sigma_{x,y,z} \approx$ 1cm & $\sigma_t$ < 150 ps

double plane 11 during bar mounting

## Design goals:

- >90% efficiency for 0.2-1.0 GeV neutrons
- multi-hit capability for up to 5 neutrons
- invariant mass resolution down to $\Delta E$ < 20 keV at 100 keV above thr.



Courtesy of K. Boretzky

# Tracking Detectors: TOF Wall

- Size: 120 x 100 cm²
- Total of 176 paddles, arranged into 4 layers
- No light guide, PMT R8619 coupled directly to scintillator
- Movable holding structure to sweep TOF wall across beam

| | |
|---|---|
| Z separation | $\sigma_E < 1\%$ |
| A separation | $\sigma_t < 38$ ps |
| Rate | 1 MHz |

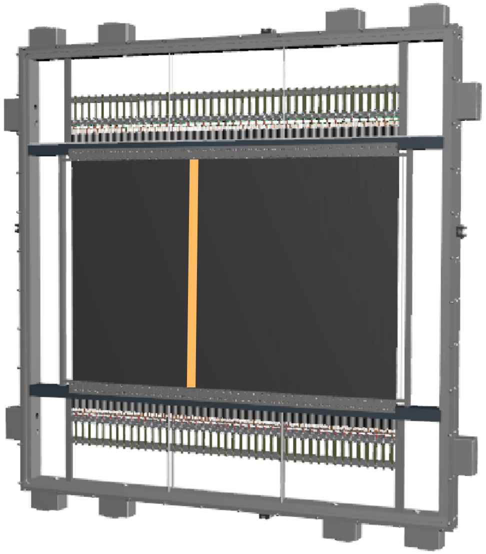

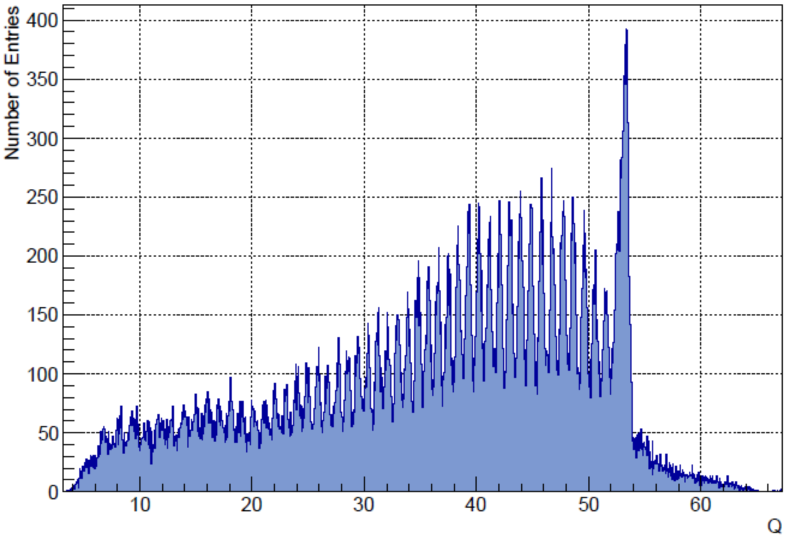


Courtesy of M. Heil

# BECOLA experimental setup

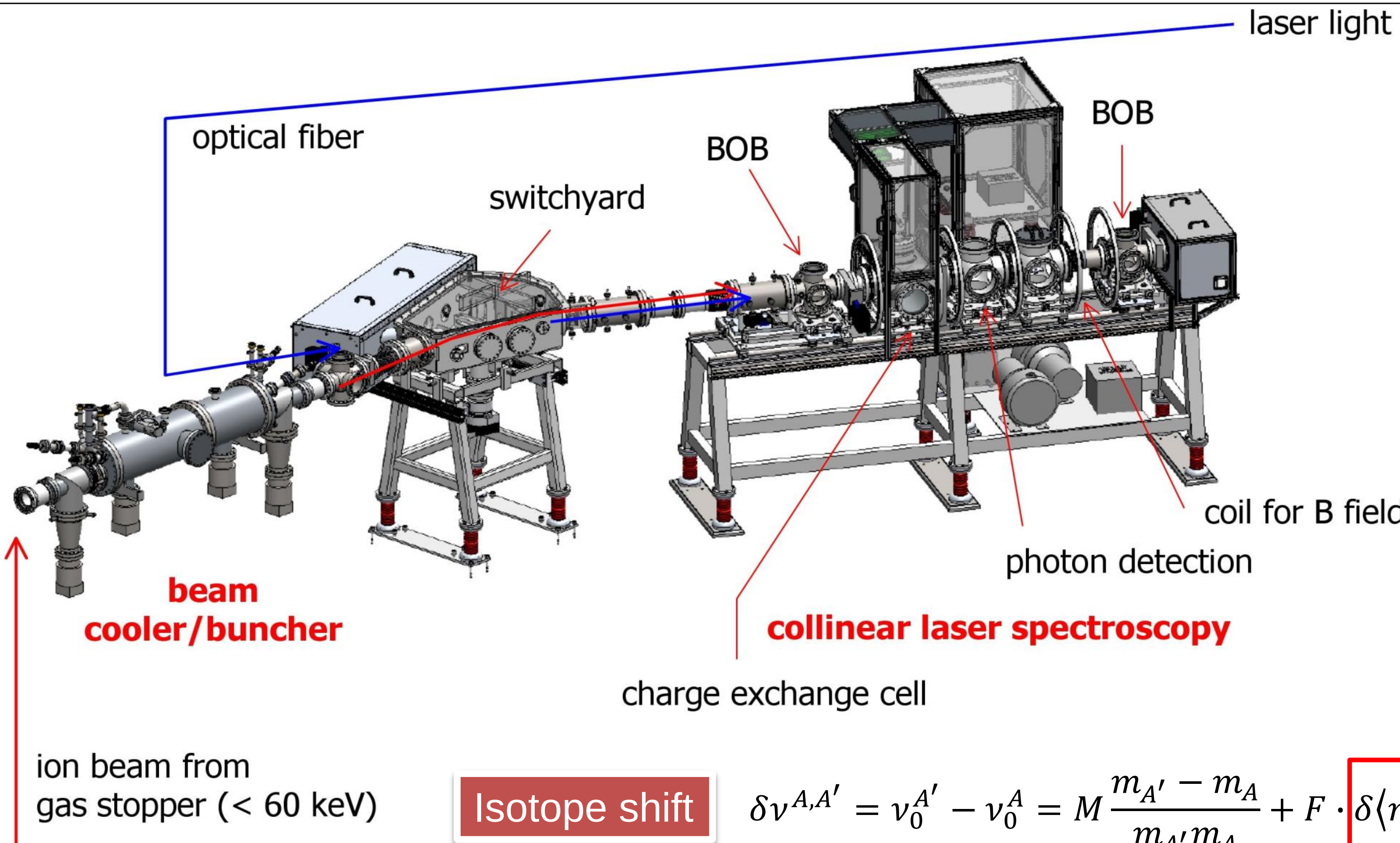


Isotope shift

$$\delta\nu^{A,A'} = \nu_0^{A'} - \nu_0^{A} = M\frac{m_{A'} - m_A}{m_{A'} m_A} + F \cdot \delta\langle r_{ch}^2\rangle^{A,A'}$$

# Coupled cyclotron facility layout

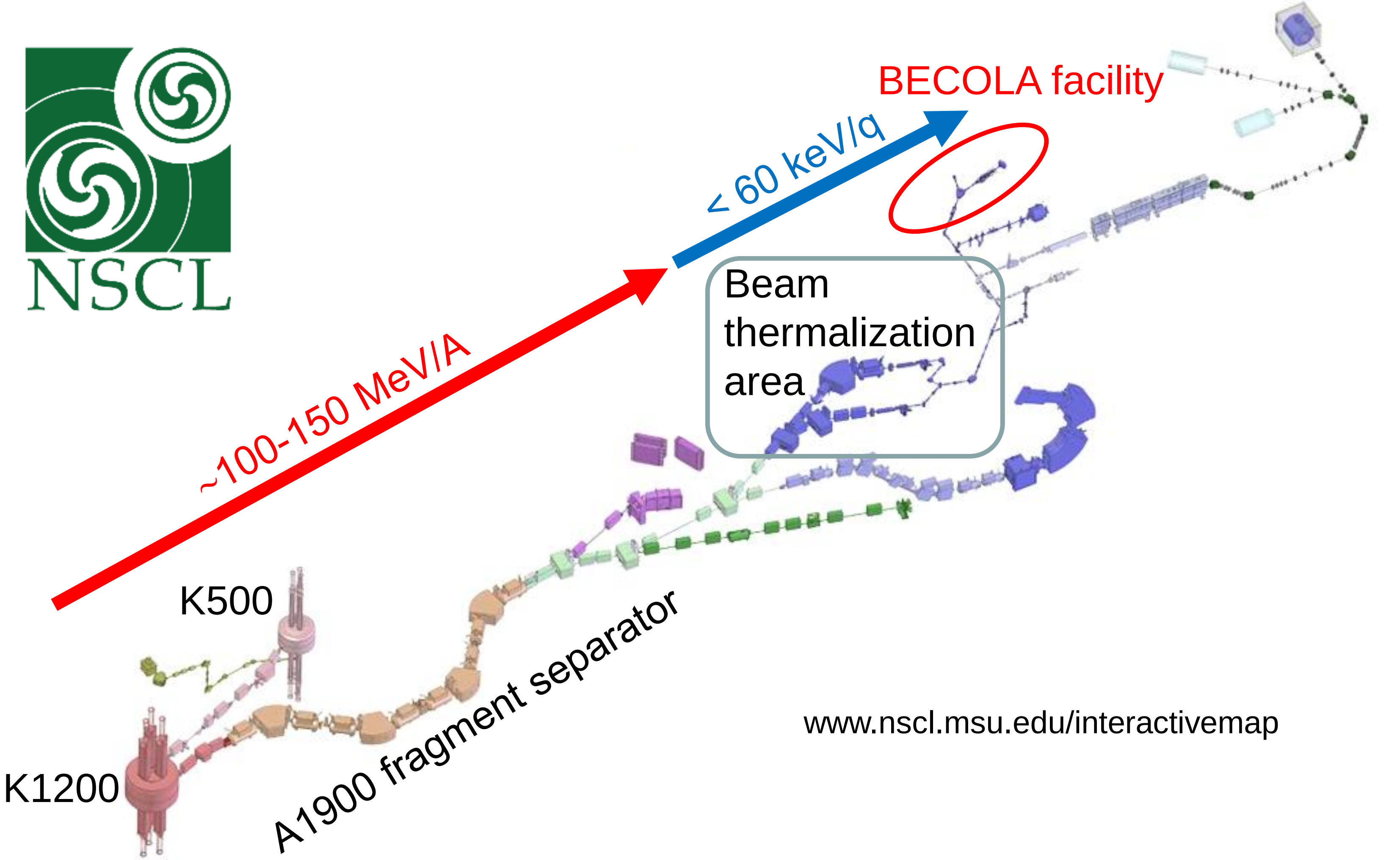


www.nscl.msu.edu/interactivemap

# Connection to nuclear symmetry energy

TECHNISCHE UNIVERSITÄT DARMSTADT

$$\Delta R_{np} \equiv R_n(Z,N) - R_p(Z,N) \overset{c.s.}{\longrightarrow} R_p(N,Z) - R_p(Z,N) \equiv \Delta R_{ch}$$

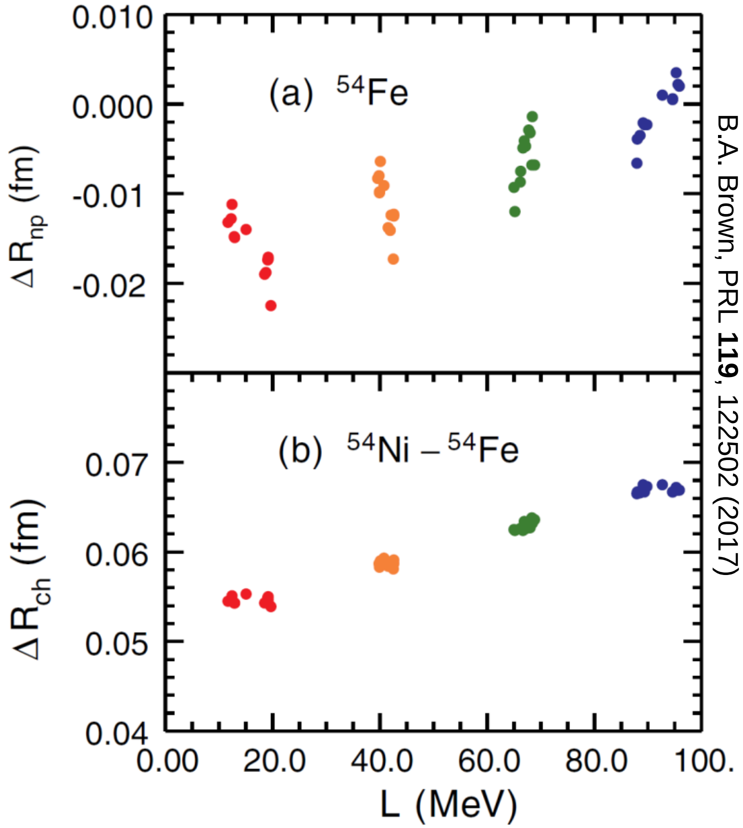


- Correlations of 48 Skyrme functionals between neutron-skin thickness $\Delta R_{n,p}$, mirror charge radius difference $\Delta R_{ch}$ and L
- In perfect charge symmetry, the neutron radius of a given nucleus equals the proton radius of its mirror nucleus
- Theoretical challenge to correctly include Coulomb corrections
- Measurement of charge radii of radioactive nuclei to the order of 0.001 fm

→ Error on isotope shift in MHz range (feasible)

→ Error on mass and field shift parameters (atomic theory) often larger (up to 1 order of magnitude)

# Connection to nuclear symmetry energy

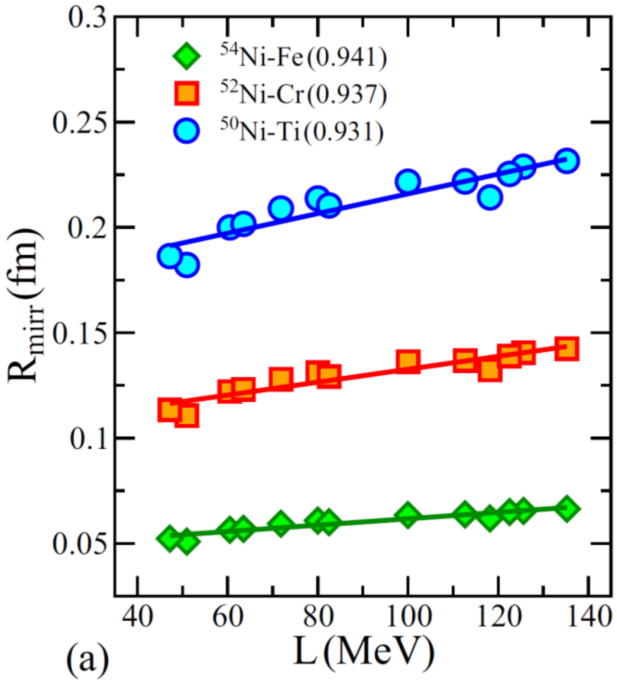


J. Wang and J. Piekarewicz, PRC **97**, 014314 (2018)

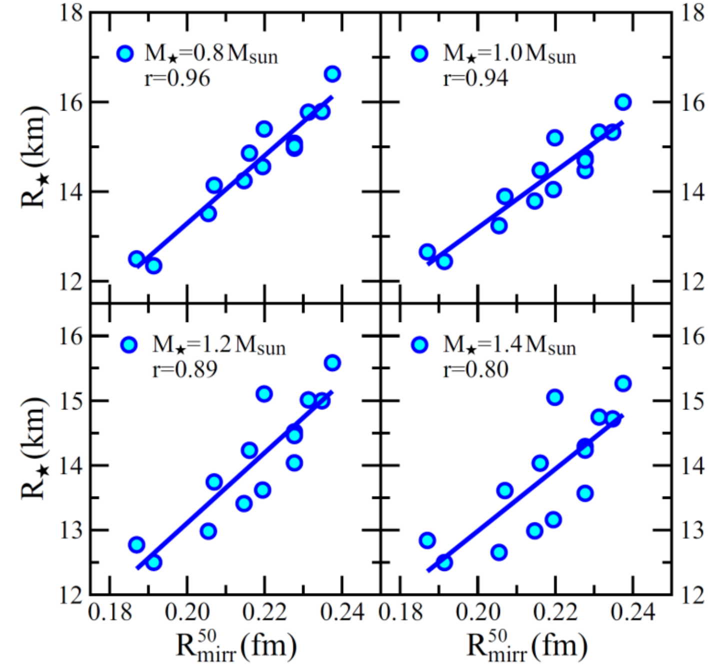


J. Wang and J. Piekarewicz, PRC **97**, 014314 (2018)

- Same behavior observed with RMF calculations
- Strong linear correlation between mirror charge difference and L leads to exploration of correlations with neutron-star radii

# Summary

- Dipole polarizability data analysis still ongoing for n-rich Sn and Ni isotopes
- Extraction of E1 strength below neutron threshold in $^{132}$Sn in progress

- Multiple experimental challenges to be overcome for future $\alpha_D$ measurements
- Key detectors for polarizability studies will be finalized and commissioned in the near future

- New approach using mirror charge radii of $^{54}$Ni-$^{54}$Fe to constrain symmetry energy

# The R3B Collaboration

TECHNISCHE UNIVERSITÄT DARMSTADT

Aksouh, Farouk; Al-Khalili, Jim; Algora, Alejandro; Alkhasov, Georgij; Altstadt, Sebastian; Alvarez, Hector; Atar, Leyla; Audouin, Laurent; Aumann, Thomas; Pellereau, Eric; Martin, Julie-Fiona; Gorbinet, Thomas; Seddon, Dave; Kogimtzis, Mos; Avdeichikov, Vladimir; Barton, Charles; Bayram, Murat; Belier, Gilbert; Bemmerer, Daniel; Michael Bendel; Benlliure, Jose; Bertulani, Carlos; Bhattacharya, Sudeb; Bhattacharya, Chandana; Le Bleis, Tudi; Boilley, David; Boretzky, Konstanze; Borge, Maria Jose; Botvina, Alexander; Boudard, Alain; Boutoux, Guillaume; Boehmer, Michael; Caesar, Christoph; Calvino, Francisco; Casarejos, Enrique; Catford, Wilton; Cederkall, Joakim; Cederwall, Bo; Chapman, Robert; Alexandre Charpy; Chartier, Marielle; Chatillon, Audrey; Chen, Ruofu; Christophe, Mayri; Chulkov, Leonid; Coleman-Smith, Patrick; Cortina, Dolores; Crespo, Raquel; Csatlos, Margit; Cullen, David; Czech, Bronislaw; Danilin, Boris; Davinson, Tom; Paloma Diaz; Dillmann, Iris; Fernandez Dominguez, Beatriz; Ducret, Jean-Eric; Duran, Ignacio; Egelhof, Peter; Elekes, Zoltan; Emling, Hans; Enders, Joachim; Eremin, Vladimir; Ershov, Sergey N.; Ershova, Olga; Eronen, Simo; Estrade, Alfredo; Faestermann, Thomas; Fedorov, Dmitri; Feldmeier, Hans; Le Fevre, Arnaud; Fomichev, Andrey; Forssen, Christian; Freeman, Sean; Freer, Martin; Friese, Juergen; Fynbo, Hans; Gacsi, Zoltan; Garrido, Eduardo; Gasparic, Igor; Gastineau, Bernard; Geissel, Hans; Gelletly, William; Genolini, B.; Gerl, Juergen; Gernhaeuser, Roman; Golovkov, Mikhail; Golubev, Pavel; Grant, Alan; Grigorenko, Leonid; Grosse, Eckart; Gulyas, Janos; Goebel, Kathrin; Gorska, Magdalena; Haas, Oliver Sebastian; Haiduc, Maria; Hasegan, Dumitru; Heftrich, Tanja; Heil, Michael; Heine, Marcel; Heinz, Andreas; Ana Henriques; Hoffmann, Jan; Holl, Matthias; Hunyadi, Matyas; Ignatov, Alexander; Ignatyuk, Anatoly V.; Ilie, Cherciu Madalin; Isaak, Johann; Isaksson, Lennart; Jakobsson, Bo; Jensen, Aksel; Johansen, Jacob; Johansson, Hakan; Johnson, Ron; Jonson, Bjoern; Junghans, Arnd; Jurado, Beatriz; Jaehrling, Simon; Kailas, S.; Kalantar, Nasser; Kalliopuska, Juha; Kanungo, Rituparna; Kelic-Heil, Aleksandra; Kezzar, Khalid; Khanzadeev, Alexei; Kissel, Robert; Kisselev, Oleg; Klimkiewicz, Adam; Kmiecik, Maria; Koerper, Daniel; Kojouharov, Ivan; Korsheninnikov, Alexei; Korten, Wolfram; Krasznahorkay, Attila; Kratz, Jens Volker; Kresan, Dima; Anatoli Krivchitch; Kroell, Thorsten; Krupko, Sergey; Kruecken, Reiner; Kulessa, Reinhard; Kurz, Nikolaus; Kuzmin, Eugenii; Labiche, Marc; Langanke, Karl-Heinz; Langer, Christoph; Lapoux, Valerie; Larsson, Kristian; Laurent, Benoit; Lazarus, Ian; Le, Xuan Chung; Leifels, Yvonne; Lemmon, Roy; Lenske, Horst; Lepine-Szily, Alinka; Leray, Sylvie; Letts, Simon; Li, Songlin; Liang, Xiaoying; Lindberg, Simon; Lindsay, Scott; Litvinov, Yuri; Lukasik, Jerzy; Loeher, Bastian; Mahata, Kripamay; Maj, Adam; Marganiec, Justyna; Meister, Mikael; Mittig, Wolfgang; Movsesyan, Alina; Mutterer, Manfred; Muentz, Christian; Nacher, Enrique; Najafi, Ali; Nakamura, Takashi; Neff, Thomas; Nilsson, Thomas; Nociforo, Chiara; Nolan, Paul; Nolen, Jerry; Nyman, Goran; Obertelli, Alexandre; Obradors, Diego; Ogloblin, Aleksey; Oi, Makito; Palit, Rudrajyoti; Panin, Valerii; Paradela, Carlos; Paschalis, Stefanos; Pawlowski, Piotr; Petri, Marina; Pietralla, Norbert; Pietras, Ben; Pietri, Stephane; Plag, Ralf; Podolyak, Zsolt; Pollacco, Emanuel; Potlog, Mihai; Datta Pramanik, Ushasi; Prasad, Rajeshwari; Fraile Prieto, Luis Mario; Pucknell, Vic; Galaviz -Redondo, Daniel; Regan, Patrick; Reifarth, Rene; Reinhardt, Tobias; Reiter, Peter; Rejmund, Fanny; Ricciardi, Maria Valentina; Richter, Achim; Rigollet, Catherine; Riisager, Karsten; Rodin, Alexander; Rossi, Dominic; Roussel-Chomaz, Patricia; Gonzalez Rozas, Yago; Rubio, Berta; Roeder, Marko; Saito, Takehiko; Salsac, Marie-Delphine; Rodriguez Sanchez, Jose Luis; Santosh, Chakraborty; Savajols, Herve; Savran, Deniz; Scheit, Heiko; Schindler, Fabia; Schmidt, Karl-Heinz; Schmitt, Christelle; Schnorrenberger, Linda; Schrieder, Gerhard; Schrock, Philipp; Sharma, Manoj Kumar; Sherrill, Bradley; Shrivastava, Aradhana; Shulgina, Natalia; Sidorchuk, Sergey; Silva, Joel; Simenel, Cedric; Simon, Haik; Simpson, John; Singh, Pushpendra Pal; Sonnabend, Kerstin; Spohr, Klaus; Stanoiu, Mihai; Stevenson, Paul; Strachan, Jon; Streicher, Brano; Stroth, Joachim; Syndikus, Ina; Suemmerer, Klaus; Taieb, Julien; Tain, Jose L.; Tanihata, Isao; Tashenov, Stanislav; Tassan-Got, Laurent; Tengblad, Olof; Teubig, Pamela; Thies, Ronja; Togano, Yasuhiro; Tostevin, Jeffrey A.; Trautmann, Wolfgang; Tuboltsev, Yuri; Turrion, Manuela; Typel, Stefan; Udias-Moinelo, Jose; Vaagen, Jan; Velho, Paulo; Verbitskaya, Elena; Veselsky, Martin; Wagner, Andreas; Walus, Wladyslaw; Wamers, Felix; Weick, Helmut; Wimmer, Christine; Winfield, John; Winkler, Martin; Woods, Phil; Xu, Hushan; Yakorev, Dmitry; Zegers, Remco; Zhang, Yu-Hu; Zhukov, Mikhail; Zieblinski, Miroslaw; Zilges, Andreas;

# BECOLA Collaboration

PHY-11-02511
PHY-12-28489

DE-NA0002924